# Discrimination of Cardiac Subcellular Creatine Kinase Fluxes by NMR Spectroscopy: A New Method of Analysis

Frédéric Joubert, Jacqueline A. Hoerter, and Jean-Luc Mazet

Institut National de la Santé et de la Recherche Médicale U-446, Cardiologie Cellulaire et Moléculaire, Université Paris-Sud, Faculté de Pharmacie, 92296 Châtenay-Malabry, France

ABSTRACT   A challenge in the understanding of creatine kinase (CK) fluxes reflected by NMR magnetization transfer in the perfused rat heart is the choice of a kinetic model of analysis. The complexity of the energetic pathways, due to the presence of adenosine triphosphate (ATP)–inorganic phosphate (Pi) exchange, of metabolite compartmentation and of subcellular localization of CK isozymes cannot be resolve from the sole information obtained from a single NMR protocol. To analyze multicompartment exchanges, we propose a new strategy based on the simultaneous analysis of four inversion transfer protocols. The time course of ATP and Phosphocreatine (PCr) magnetizations computed from the McConnell equations were adjusted to their experimental value for exchange networks of increasing complexity (up to six metabolite pools). Exchange schemes were selected by the quality of their fit and their consistency with data from other sources: the size of mitochondrial pools and the ATP synthesis flux. The consideration of ATP–Pi exchange and of ATP compartmentation were insufficient to describe the data. The most appropriate exchange scheme in our normoxic heart involved the discrimination of three specific CK activities (cytosolic, mitochondrial, and close to ATPases). At the present level of heart contractility, the energy is transferred from mitochondria to myofibrils mainly by PCr.

## INTRODUCTION

The kinetics of the creatine kinase reaction (CK) (adenosine triphosphate (ATP) creatine phosphotransferase, E.C. 2.7.3.2), which catalyzes the reversible exchange of high-energy phosphate between phosphocreatine (PCr) and ATP:

$$\text{PCr}^{2-} + \text{MgADP}^- + \text{H}^+ \xrightleftharpoons[F_r]{F_f} \text{Cr} + \text{Mg ATP}^{2-},$$
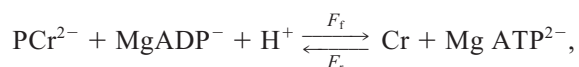
have early been studied in heart by $^{31}\text{P}$ NMR saturation transfer technique. The estimation of the forward ($F_f$: PCr→ATP) and reverse ($F_r$: ATP→PCr) fluxes initially assumed a simple two-site exchange PCr↔ATP. However, the use of this two-site scheme of exchange requires that two conditions are fulfilled: a free diffusion of the CK substrates and no implication of ATP in other exchanges. A discrepancy between the forward and reverse flux ($F_f/F_r \neq 1$) often was observed despite the myocardium working at steady-state. Such discrepancy pointed out to the limitation of this two-site exchange and has been proposed to result from a subcellular compartmentation of substrates or enzymes (Nunnally and Hollis, 1979; Koretsky et al., 1985), or from an exchange of ATP with other phosphorus species such as inorganic phosphate (Pi) (Ugurbil et al., 1986; Spencer et al., 1988). Recently, we showed by inversion transfer that both mitochondrial ATP compartmentation and ATP exchange with Pi contribute to this apparent myocar-

dial flux discrepancy (Joubert et al., 2000). A four-site exchange scheme was needed to describe the CK kinetics using an inversion transfer protocol under continuous saturation of Pi (a procedure masking the influence of the ATP↔Pi flux). It was, however, still insufficient to fully account for the NMR data obtained without saturation of Pi and to reflect the myocardial energetic exchanges (Joubert et al., 2001).

The myocardial cell has a complex organization due to the intracellular localization of its CK isoforms. Indeed, half of the total CK is cytosolic, whereas the other half is located in the vicinity of myofibrillar, sarcoplasmic reticular, and sarcolemmal ATPases (MM-CK isoform) and of the adenine translocator (mitochondrial CK [mito-CK] isoform). In vitro or in skinned fibers, such vicinity influences the enzyme kinetics (Saks et al., 1985; Ventura-Clapier et al., 1987; Arrio-Dupont et al., 1992). This type of localization of CK isoforms is a characteristic of the highly organized adult cardiomyocyte, contributes to its efficiency, and is thought to play a crucial role in energy transfer (for review, see Wallimann et al., 1992; Saks et al., 1996). As pointed out by Wallimann (1996), the understanding of the CK function might be greatly limited when the cell is considered a homogenous system where enzymes and metabolites have uniform concentrations, in other words, when using simplistic schemes of exchange for NMR data analysis.

Thus, a major challenge in the interpretation of NMR data in the whole organ is the choice of a kinetic model of analysis. Only simple schemes can be used when a single magnetization transfer protocol is performed, because only a small number of kinetic parameters can be adjusted (at most two in a saturation and four in an inversion protocol). In this condition, the complex cellular organization is beyond the potentiality of NMR. We suggest here that a

Address reprint requests to Jean-Luc Mazet U-446 INSERM, Cardiologie Cellulaire et Moléculaire, Faculté de Pharmacie, 5 rue J.-B. Clément, 92296 Châtenay-Malabry, France. Tel.: +33-1-46835769; Fax: +33-1-46835475; E-mail: jean-luc.mazet@cep.u-psud.fr.

simultaneous analysis of different protocols of inversion (inv-PCr, inv-ATP with or without saturation of Pi) could allow the test of more complex kinetic exchanges and thus bring detailed insight on the energy fluxes in the myocardial cell.

Our strategy was to find the best scheme of energetic pathways for a heart in moderate working conditions from the comparison of the time evolution of magnetization under the NMR inversion protocols with their theoretical evolution predicted from the resolution of Bloch equations describing the different structures of exchange between compartments. We do not compute the CK kinetics, but we use magnetization transfer of the phosphate moiety as a tracer of myocardial energetic fluxes. First, we analyzed the data in a simple three-site scheme of exchange PCr↔ATP↔Pi. Next, we introduced an additional ATP compartment (of which the mitochondrial localization is discussed) and its exchange with cytosolic metabolites. Finally, an ATP compartment in the vicinity of the sites of ATP utilization was added. A minimal exchange scheme was selected on the basis of three criteria: 1) the use of the smallest number of parameters necessary to describe the kinetic exchanges of phosphorus species by NMR; 2) a steady state of the global CK metabolites ($F_f$ must theoretically equal $F_r$); and 3) the quality of the fit. Finally, the choice of exchange schemes was validated by comparison with experimental estimates of the size of fluxes and metabolic pools measured by other techniques such as oxygen consumption and subcellular fractionation.

## METHODS

### Experimental

#### Physiology

This investigation conforms with INSERM guidelines, which are defined by the European Community guiding principles in the care and use of animals and the French decree #87/84, Oct. 19, 1987. Authorization to perform animal experiments according to this decree was obtained from the French Ministère de l'Agriculture de la Pêche et de l'Alimentation (#7473, 1997). Hearts of Wistar male rats (350–450 g) were perfused by the Langendorff technique at a constant flow (13.5 ml/min). A latex balloon, inserted in the left ventricle, was inflated to isovolumic conditions of work and allowed to record the contractile parameters (Stepanov et al., 1997). The HEPES-buffered perfusate contained Na-acetate, 10 mM, as oxidative substrate to minimize the activity of glycolysis. Contractility was characterized by the mean coronary pressure, left ventricle systolic pressure, end diastolic pressure, heart spontaneous frequency, and rate pressure product (in $10^4$ mmHg·beats/min). For each heart, the oxygen consumption ($QO_2$) was inferred from the relationship between contractility and $QO_2$ (Stepanov et al., 1997).

#### NMR protocols

^{31}P NMR spectra were acquired at 161.93 MHz on an INOVA Varian wide-bore magnet in a 20-mm-diameter tube (Joubert et al., 2000). Control spectra were obtained with an 80° pulse angle, 4 K data points acquisition, a spectral width of 10,000 Hz, and a line broadening of 20 Hz. Fully relaxed spectra (repetition time 10 s) were acquired before

and after each inversion experiment. Selective inversion of either PCr (inv-PCr), or γATP (inv-ATP) was achieved by a sinc pulse of 15 ms followed by a variable delay (0 to 10 s, $n = 14$) before the sampling pulse and a 10-s delay for complete relaxation. Twenty-four scans were required (four scans cycling six times through the whole protocol). Inv-PCr and Inv-ATP protocols were additionally performed with a continuous saturation of Pi resonance by a selective pulse (Joubert et al., 2000). In all groups the hearts were in steady state. For each heart the magnetizations of ATP and PCr were followed over time. The size of the Pi resonance was too small in acetate substrate to allow the experimental determination of its time course during the inversion protocol. At the end of the NMR experiments, all the hearts were freeze clamped. A part of the frozen hearts was used to measure ATP, PCr, and creatine contents (in nmoles/mg protein) and to calculate the metabolite concentrations during magnetization transfer. All data were expressed in mmol l of intracellular water, assuming 2.72 $\mu$l $H_2O$/mg protein (Hoerter et al., 1988; Stepanov et al., 1997). For each inversion protocol, five or six hearts were used, the time courses of the evolution of ATP and PCr were averaged for the global analysis.

### Analysis

The classical analysis of tracer experiments was used to describe the measurement of phosphate exchange between nucleotides by NMR methods. In a system at equilibrium, such an analysis is based on a multicompartment and exchange flux representation. The resultant theoretical kinetics are described by a sum of exponential. The parameters of each exponential depend only on the compartment organization and on the experimental protocol. For a given structure of compartmentation, the values of the exponential parameters fitting the kinetics varies with the applied NMR protocol, because the inversion transfer protocols do not trace the same fluxes in the presence or the absence of Pi saturation. However, independent of the applied experimental protocol, the exponential parameters reflects the properties of the same unidirectional fluxes between the compartments, because we are dealing with the same steady state. This implies that the exponential parameters derived from a single protocol are not independent of those derived from other protocols. Only a few parameters may be calculated in a single protocol: at most four in an inversion transfer and only two in a time-dependent saturation transfer protocol. On the contrary, fitting simultaneously the parameters to several protocols makes it possible to compute a larger number of parameters and thus to resolve more complex schemes of exchange. In the present work, we propose to fit each scheme of exchange under test to the four NMR protocols together: Inv-PCr and Inv-ATP, both in the presence and the absence of Pi saturation.

#### Data analysis

In a given scheme of kinetic exchange, the theoretical time responses of ATP, PCr, and Pi magnetizations were computed from the McConnell equations for all the inversion protocols. Obviously the matrix describing the time evolution of magnetization increased in complexity when additional compartments and their exchange were considered. The deviation of the theoretical time response from the averaged NMR data was calculated by the $\chi^2$ function,

$$\chi^2 = \sum_{i=1}^{N} \left( \frac{ATP_i - f(t_i; a_1 \ldots a_P)}{\sigma_{ATP}} \right)^2$$

$$+ \sum_{i=1}^{N} \left( \frac{PCr_i - g(t_i; a_1 \ldots a_P)}{\sigma_{PCr}} \right)^2$$

where $ATP_i$ and $PCr_i$ are the averaged experimental data points at each time $t_i$ (ranging from 1 to $N = 112$) with their own standard error $\sigma$. For each

species, ATP and PCr, a unique $\sigma$ value was used, which included the NMR measurement error and the SEM. of the averaged data ($\sigma_{ATP} = 0.19$ and $\sigma_{PCr} = 0.18$). $f$ and $g$ are the theoretical values of the ATP and PCr magnetization for each time $t_i$. The set of parameters ($a_1 \ldots a_p$), describing the size of the metabolic pools, the unidirectional fluxes and the time constants $T_1$ of relaxation, ranged from 5 to 9 depending on the exchange scheme. For each scheme, the parameters ($a_1 \ldots a_p$) were adjusted to minimize the $\chi^2$ function. When this was obtained, the min $\chi^2$ and the fitted parameters were reported with their confidence interval at 68.3% estimated from the correlation matrix as the square root of their autocovariance ($C_{1,1} \ldots C_{p,p}$), assuming a normal error distribution. The confidence interval of the CK flux ratio $R$ ($= F_f/F_r$) was derived by the formula,

$$\frac{\delta R}{R} = \sqrt{\left(\frac{\delta F_f}{F_f}\right)^2 + \left(\frac{\delta F_r}{F_r}\right)^2 - 2\Theta \left(\frac{\delta F_f}{F_f}\right)\left(\frac{\delta F_r}{F_r}\right)},$$

with $\Theta$ defined from the correlation matrix as

$$\Theta = \frac{C_{F_f F_r}}{\sqrt{C_{F_f} C_{F_r}}}.$$

### Description of the program

The fitting program, called NORFIT, was written and compiled in our laboratory with LabVIEW 5 (National Instruments Corp., Austin, TX) and can be obtained from J.-L. Mazet. The inputs for the program were read from EXCEL7 (Microsoft, Redmont, CA) worksheets. In the data part, the four inversion protocols were combined into: 1) one set containing the NMR data ($\gamma$ATP and PCr magnetization variations as a function of the mixing time, and their standard errors); and 2) a second set describing quantitatively the imposed protocols of magnetization. The model part contained the pools, the unidirectional fluxes, and the demagnetization parameters of all compartments. Each parameter was initially described by its input value and a code defining the constraints of the model (Fig. 1). The main loop (*thick arrows*) includes an algorithm calculating the response (from the initial parameter set and the protocol), through the theoretical equations of McConnell (1958) describing the evolutions of the magnetization. This response was compared with the experimental data in a program module that computes $\chi^2$ and the covariance

matrix. From these parameters, a new set of parameters was estimated by the method of Levenberg–Marquardt (Press et al., 1994). The loop was carried on until $\chi^2$ reached a minimum, min $\chi^2$, each output parameter is then given with its interval of confidence.

To limit the number of parameters to be adjusted, only compartment organizations reasonably consistent with the physiological knowledge of energetic exchanges were investigated. In a preliminary step of computation, the number of adjustable parameters was kept small by adding some constraints to the scheme to find initial values of the parameters and prevent the algorithm from diverging. Then the constraints were progressively released to increase the number of adjustable parameters. As expected, the fit was improved as the number of adjustable parameters increased. Beyond some threshold number, the min $\chi^2$ was not further improved, but the confidence interval of some parameters, i.e., the incertitude on their determination, tended to increase dramatically, and eventually the algorithm became divergent. This threshold number was $\sim 8$–9 parameters, depending on the structure of the exchange scheme, and set a limit to the choice of a minimal scheme.

### Strategy of analysis

A particular attention was devoted to the equality of the total forward and reverse fluxes. For this, two different approaches were used. At first, the equality of $F_f$ and $F_r$ was not imposed, the only constraints were the total cellular amount of each metabolite and the similarity of $T_1$ of each species in all its compartments. When a reasonable agreement was reached between $F_f$ and $F_r$ (see Results), we assumed that more complex schemes were of no use. This step was used for a rough selection of relevant schemes of exchange. In the second approach, the real steady state, total $F_f$ = total $F_r$, was imposed as additional constraint and the exchange schemes were evaluated on the basis of the quality of their fit. Finally, the adequacy of the fitted parameters to the measured values of the mitochondrial ATP synthesis (estimated from oxygen consumption) and of the size of the ATP$_2$ compartment (estimated by subcellular fractionation, Joubert et al., 2001) was also considered as a criterion of choice and allowed to propose a physiological identification of the kinetic compartments.

## RESULTS

### Experimental data

Contractile and metabolic characteristics of the hearts are shown in Table 1 for the four inversion protocols. Because all values were similar, all the data were pooled for the analysis. Figure 2 shows a typical set of NMR data and their analysis. The four protocols: inv-PCr, inv-ATP, with and without saturation of Pi resonance were queued. The time evolution of PCr and ATP magnetization (mean $\pm$ SE of five hearts, measured for each inversion protocol) is shown in symbols, and the theoretical response according to a scheme of exchange is shown in lines.

### The apparent forward-to-reverse flux discrepancy results from the use of a simplistic scheme of exchange

At this step of analysis, the global balance of CK fluxes was not imposed. Because the heart is in a steady state and PCr is only involved in exchanges through CK reactions, $F_f$ is expected to equal $F_r$. Table 2 shows the main exchange schemes
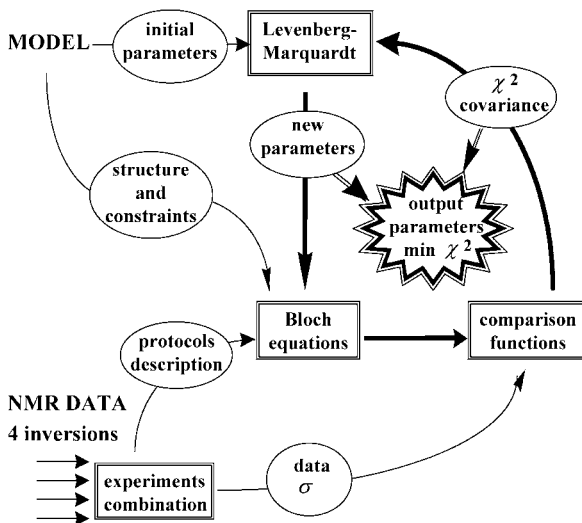


FIGURE 1  Structure of NORFIT. The rectangles symbolize the program modules and the ellipses the data or parameter sets.

**TABLE 1  Contractile and metabolic characteristics of perfused hearts**

|  | $n$ | PCr | ATP | Pi | LVP | Heart Rate | CP | RPP |
|---|---|---|---|---|---|---|---|---|
| Inv-PCr | 5 | $11.9 \pm 0.5$ | $7.1 \pm 0.7$ | $2.5 \pm 0.4$ | $154 \pm 9$ | $271 \pm 10$ | $58 \pm 1$ | $4.2 \pm 0.3$ |
| Inv-ATP | 5 | $11.4 \pm 0.5$ | $6.1 \pm 0.4$ | $2.9 \pm 0.3$ | $152 \pm 5$ | $271 \pm 14$ | $52 \pm 1$ | $4.1 \pm 0.2$ |
| Inv-PCr satPi | 5 | $12.8 \pm 0.5$ | $7.4 \pm 0.7$ | $2.7 \pm 0.3$ | $135 \pm 8$ | $279 \pm 10$ | $60 \pm 2$ | $3.8 \pm 0.3$ |
| Inv-ATP satPi | 5 | $12.9 \pm 0.2$ | $6.5 \pm 0.3$ | $2.6 \pm 0.3$ | $149 \pm 9$ | $265 \pm 11$ | $60 \pm 1$ | $3.9 \pm 0.3$ |
| Mean | 20 | $12.3 \pm 0.3$ | $6.8 \pm 0.3$ | $2.9 \pm 0.2$ | $148 \pm 4$ | $271 \pm 6$ | $60 \pm 1$ | $4.0 \pm 0.1$ |

Metabolic concentrations (PCr, ATP, Pi) expressed in mmoles/1 $H_2O$, systolic (LVP) and coronary pressure (CP) in mmHg, heart rate in beats/min, and rate pressure product (RPP = LVP $\times$ heart rate) in $10^4$ mmHg beats/min. End diastolic pressure was unchanged during the magnetization transfer protocols (initial value: 5–8 mmHg). Mean intracellular pH was $7.09 \pm 0.01$ and the PCr-to-ATP ratio $1.82 \pm 0.10$. Oxygen consumption was $10.1 \pm 0.3$ $\mu$mol $O_2$/min·gWW. ATP synthesis, calculated from $QO_2$ (assuming a P/O ratio of 6, and an intracellular volume of 435 $\mu$L $H_2O$·gWW) was $2.3 \pm 0.1$ mmoles/1/s.

under test and the value of the forward-to-reverse flux ratio for each exchange structure. The experimental data were first compared to the simplest three-site exchange (scheme 1 in Table 2): $F_f/F_r$ significantly differed from unity ($0.75 \pm 0.05$). Such an apparent flux discrepancy between $F_f$ and $F_r$ confirmed our previous observations that the consideration of only one CK flux and an ATP↔Pi exchange, was inadequate to fully describe myocardial energy exchanges.

Exchanges of increasing complexity were then tested. An additional ATP compartment ($ATP_2$) was first introduced.

Its presence, either isolated from Pi and PCr (scheme 2), or exchanging with Pi via $ATP_2$↔Pi (scheme 3) did not abolished the apparent flux discrepancy ($F_f/F_r$ was $0.83 \pm 0.08$ and $0.80 \pm 0.10$, respectively). Similarly, scheme 4, which
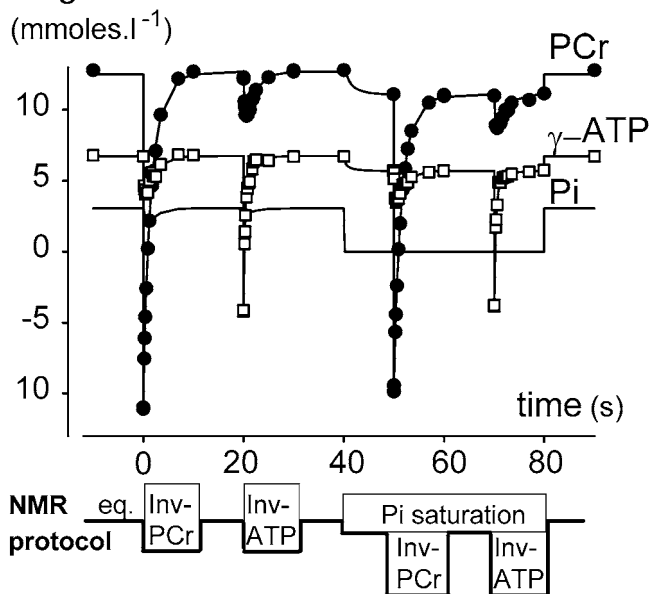
## Magnetization
$(mmoles.l^{-1})$



FIGURE 2  Inversion NMR data and analysis. After an equilibration period (*eq.*) corresponding to the steady-state magnetization in the absence of any inversion perturbation, the four inversion transfer protocols: inversion PCr and inversion $\gamma$ATP with and without Pi saturation, were queued. An artificial delay was introduced between each inversion protocol to improve the visualization. The evolution of PCr and ATP measured by NMR (*symbols*: mean $\pm$ SE, in mmoles/$l^{-1}$ $H_2O$) and their fitted value in the scheme 6b (*lines*) are shown as a function of the mixing time. The time evolution of Pi resonance was not directly observable; only its calculated value is shown.

**TABLE 2  First evaluation of the different exchange schemes based on $F_f/F_r$**

| No. | Scheme | $F_f/F_r$ |
|---|---|---|
| 1 | PCr⇌ATP⇌Pi | 0.75 (0.05)* |
| 2 | PCr⇌$ATP_1$⇌Pi<br>$ATP_2$ | 0.83 (0.08)[†] |
| 3 | PCr⇌$ATP_1$⇌Pi<br>⤢<br>$ATP_2$ | 0.80 (0.10)[†] |
| 4 | PCr⇌$ATP_1$→Pi<br>↑  ↙<br>$ATP_2$ | 0.78 (0.08)[†] |
| 5 | PCr⇌$ATP_1$→Pi<br>↖  ↙<br>$ATP_2$ | 0.79 (0.09)[†] |
| 5b | $PCr_1$⇌$ATP_1$→Pi<br>↖  ↙<br>$PCr_2$  $ATP_2$ | 0.78 (0.09)[†] |
| 5c | $PCr_1$⇌$ATP_1$→Pi<br>↑  ↙<br>$PCr_2$←$ATP_2$ | 0.77 (0.12)[†] |
| 6 | $ATP_3$<br>↗  ↘<br>PCr⇌$ATP_1$  Pi<br>↖  ↙<br>$ATP_2$ | 0.90 (0.32) |
| 6b | $ATP_3$<br>↗  ↘<br>PCr⇌$ATP_1$  Pi<br>↖<br>$PCr_2$  $ATP_2$ | 0.92 (0.33) |

Because metabolites are in a steady state, we compared the flux ratio $F_f/F_r$ to 1 by using the confidence interval of the flux ratio (see Methods).
*The difference between $F_f/F_r$ and 1 amounts to five times the confidence interval.
[†]The difference between the flux ratio and 1 is ~2 times the confidence interval.

**TABLE 3 Dynamic parameters and size of the metabolite pools of the various schemes (global steady state imposed)**

| Scheme No. | CK Fluxes (mmoles/l $H_2O$/s) | | | | ATPase Fluxes (mmoles/1 $H_2O$/s) | | | Relaxation Parameters (s) | | Size of Pools (% of total) | | |
|---|---|---|---|---|---|---|---|---|---|---|---|---|
| | $F_f$ $PCr_1 \rightarrow ATP_1$ | $F_r$ $ATP_1 \rightarrow PCr_1$ | $F_r$ $ATP_2 \rightarrow PCr_1$ | $F_f$ $PCr_1 \rightarrow ATP_3$ | $Pi \rightarrow ATP_2$ | $ATP_1 \rightarrow Pi$ | $ATP_3 \rightarrow Pi$ | $T_{1PCr}$ | $T_{1\gamma ATP}$ | $ATP_2$ | $ATP_3$ | $PCr_2$ |
| 1 | 7.1* | 7.1 (0.3) | – | – | – | 2.6 (0.2) | – | 3.7 (0.2) | 0.7 (0.0) | – | – | – |
| 2 | 7.9* | 7.9 (0.6) | – | – | – | 2.2 (0.2) | – | 3.4 (0.3) | 0.7 (0.1) | 30 (3) | – | – |
| 3 | 8.1* | 8.1 (0.9) | – | – | 0.1 (0.2) | 2.2 (0.2) | – | 3.4 (0.3) | 0.7 (0.1) | 32 (5) | – | – |
| 4 | 7.0* | 7.0 (0.4) | – | – | 8.2 (12.8) | 8.2* | – | 3.7 (0.3) | 1.1 (2.0) | 0 (5) | – | – |
| 5 | 6.7* | 4.4 (0.4) | 2.3* | – | 2.3 (0.1) | 2.3* | – | 3.6 (0.2) | 0.7 (0.1) | 27 (4) | – | – |
| 5b | 6.8* | 4.6 (0.5) | 2.2* | – | 2.2 (0.1) | 2.2* | – | 3.5 (0.3) | 0.7 (0.1) | 24 (4) | – | 7 (2) |
| 5c | 8.0* | 5.7 (1.0) | – | – | 2.3 (0.1) | 2.3* | – | 3.3 (1.1) | 0.7 (0.1) | 44 (5) | – | 64 (3) |
| 6 | 4.9* | 4.9 (0.6) | 2.2* | 2.2* | 2.2 (0.1) | – | 2.2* | 4.2 (0.3) | 0.7 (0.1) | 23 (4) | 3 (4) | – |
| 6b | 5.0* | 5.0 (0.6) | 2.2* | 2.2* | 2.2 (0.1) | – | 2.2* | 4.0 (0.5) | 0.7 (0.1) | 22 (4) | 3 (4) | 7 (2) |

*Flux imposed to insure the steady state of the concerned pool (see Methods). This involves:
—in all schemes: the global equality of CK fluxes
—in scheme 1, 2, and 3: flux $Pi \rightarrow ATP_1$ = flux $ATP_1 \rightarrow Pi$ and additionally in scheme 3: $ATP_2 \rightarrow Pi = Pi \rightarrow ATP_2$.
—in scheme 4: $ATP_1 \rightarrow Pi = Pi \rightarrow ATP_2 = ATP_2 \rightarrow ATP_1$
—in schemes 5 and 5b: $ATP_1 \rightarrow Pi = Pi \rightarrow ATP_2 = ATP_2 \rightarrow PCr_1$
—in scheme 5c: $ATP_1 \rightarrow Pi = Pi \rightarrow ATP_2 = ATP_2 \rightarrow PCr_2 = PCr_2 \rightarrow PCr_1$
—in scheme 6 and 6b: $ATP_3 \rightarrow Pi = Pi \rightarrow ATP_2 = ATP_2 \rightarrow PCr_1 = PCr_1 \rightarrow ATP_3$
Relaxation parameters: The equality of the magnetization relaxation parameters was imposed in the various compartments ($T_{1\gamma ATP1} = T_{1\gamma ATP2} = T_{1\gamma ATP3}$ and $T_{1PCr1} = T_{1PCr2}$).
Confidence interval of the parameters is shown in parentheses.

considered a direct exchange between ATP pools, $ATP_2 \rightarrow ATP_1$, did not result in equal CK fluxes. In scheme 5, $ATP_2$ was in exchange with PCr via a second CK reaction, $ATP_2 \rightarrow PCr_1$, and, in scheme 6, an additional ATP pool ($ATP_3$) was considered, i.e., three ATP pools exchanged with PCr via three different CK reactions. In this latter exchange, the forward and reverse fluxes were similar ($F_f/F_r = 0.90 \pm 0.32$). The presence of an additional compartment of PCr, $PCr_2$, was also considered, because both ATP and PCr subcellular compartmentation was previously evidenced (Joubert et al., 2001). This $PCr_2$ pool, either isolated (scheme 5b and 6b) or included in the energy circuit (scheme 5c), hardly modified the apparent flux discrepancy (Table 2). More complex schemes including additional fluxes between compartments have been tested but were not further considered because they did not improve the balance of the flux. This includes, for example, in scheme 5, the consideration of an exchange of $ATP_2$ with both $ATP_1$ and $PCr_1$, of an exchange $PCr_1 \rightarrow ATP_2$ or of a flux $Pi \rightarrow ATP_1$ (results not shown).

This analysis shows that quasi-steady-state conditions ($F_f/F_r$ close to one) could only be obtained from an analysis of complex schemes of exchange considering the function of three CK reactions.

## The minimal scheme of kinetic exchange describing NMR data: selection on the basis of min $\chi^2$ value

From the physiological point of view, the myocardium is globally in steady state. Thus, the expected global balance of the CK fluxes had to be imposed. Table 3 summarizes the adjusted values of CK and ATPases fluxes in the various exchange schemes, as well as the relaxation parameters and the size of the metabolite compartments resulting from the fit of NMR data. For all the schemes, the NMR intrinsic relaxation parameters were compatible, within the confi-
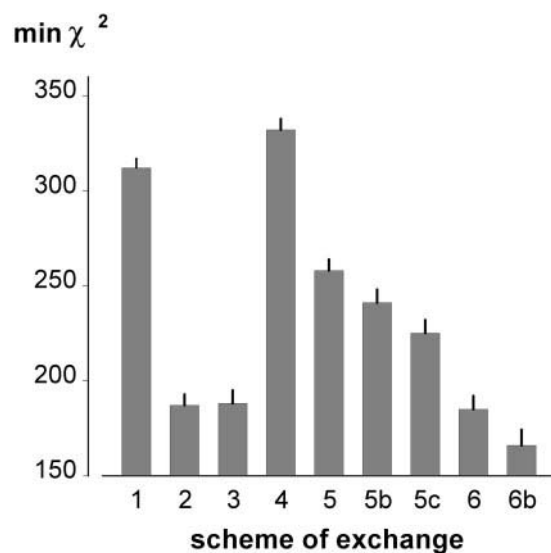


FIGURE 3 Evaluation of the various schemes of analysis based on the quality of the fit, min $\chi^2$ (steady-state imposed). The highest min $\chi^2$ were observed for schemes 1 and 4 (more than 300), whereas the lowest (the best fit of data) was found for the scheme 6b: min $\chi^2$ = 166 (8). As the number of variables increased with the complexity of the exchanges, the confidence interval increased from 5 (scheme 1) to 8 (scheme 6b). Min $\chi^2$ in schemes 1–6 were higher than in scheme 6b by more than 2 intervals of confidence.

**TABLE 4 Physiological interpretation of the kinetic schemes**

| No. | Scheme* | Exchange[†] |
|---|---|---|
| 1 | $PCr_{tot} \rightleftarrows ATP_{tot} \rightleftarrows Pi_{tot}$ | Global CK<br>Global ATP synthesis and hydrolysis |
| 2 | $PCr_{tot} \rightleftarrows ATP_{tot} \rightleftarrows Pi_{tot}$<br>$\qquad\quad ATP_{mito}$ | Global CK<br>Cyto-ATP synthesis and hydrolysis |
| 3 | $PCr_{tot} \rightleftarrows ATP_{cyto} \rightleftarrows Pi_{tot}$<br>$\qquad\quad \nwarrow\!\!\swarrow$<br>$\qquad\quad ATP_{mito}$ | Global CK<br>Cyto- and mito-ATP synthesis and hydrolysis |
| 4 | $PCr_{tot} \rightleftarrows ATP_{cyto} \rightarrow Pi_{tot}$<br>$\qquad\quad \uparrow \quad \swarrow$<br>$\qquad\quad ATP_{mito}$ | Global CK<br>Cyto-ATP hydrolysis and mito-ATP synthesis and ATP flux from mito to cyto |
| 5 | $PCr_{tot} \rightleftarrows ATP_{cyto} \rightarrow Pi_{tot}$<br>$\qquad\quad \nwarrow \quad \swarrow$<br>$\qquad\quad ATP_{mito}$ | Extramito-CK and mito-CK<br>Cyto-ATP hydrolysis and mito-ATP synthesis |
| 5b | $PCr_{cyto} \rightleftarrows ATP_{cyto} \rightarrow Pi_{tot}$<br>$\qquad\quad \nwarrow \quad \swarrow$<br>$PCr_{mito} \quad ATP_{mito}$ | Extramito-CK and mito-CK<br>Cyto-ATP hydrolysis and mito-ATP synthesis |
| 5c | $PCr_{cyto} \rightleftarrows ATP_{cyto} \rightarrow Pi_{tot}$<br>$\uparrow \qquad\qquad \swarrow$<br>$PCr_{mito} \leftarrow ATP_{mito}$ | Extramito-CK and mito-CK involving $PCr_{mito}$<br>Cyto-ATP hydrolysis and mito-ATP synthesis |
| 6 | $\qquad\quad ATP_{MM}$<br>$\qquad\nearrow \qquad \searrow$<br>$PCr_{tot} \rightleftarrows ATP_{cyto} \quad Pi_{tot}$<br>$\qquad\nwarrow \qquad \swarrow$<br>$\qquad\quad ATP_{mito}$ | Cyto-CK and mito-CK and MM bound-CK<br>$ATP_{MM}$ hydrolysis and mito-ATP synthesis |
| 6b | $\qquad\quad ATP_{MM}$<br>$\qquad\nearrow \qquad \searrow$<br>$PCr_{cyto} \rightleftarrows ATP_{cyto} \quad Pi_{tot}$<br>$\qquad\qquad \swarrow$<br>$PCr_{mito} \quad ATP_{mito}$ | Cyto-CK and mito-CK and MM bound-CK<br>$ATP_{MM}$ hydrolysis and mito-ATP synthesis |

*Subscripts tot, cyto, and mito refer to global, cytosolic, and mitochondrial metabolites, respectively. $ATP_{MM}$ (in schemes 6 and 6b), ATP pool localized in the vicinity of myofibrils or of the sarcolemma and sarcoplasmic reticulum.
[†]Global CK (in schemes 1–4), CK at all localizations (mito-, MM-bound, and cytosolic; Extramito-CK (in schemes 5, 5b, and 5c), cytosolic and MM-bound CK.

dence intervals, with published values (ranging from 0.7 to 1.1 s for $T_{1\gamma ATP}$ and from 3.3 to 4.2 s for $T_{1PCr}$). Similarly, the global CK forward flux (7–8 mmole/l/s) was in the range described in a myocardium perfused with a nonglycolytic substrate. None of these parameters could thus be used as criterion for the selection of exchange schemes.

In these conditions, the min $\chi^2$ value was the main criterion of selection. Figure 3 summarizes the min $\chi^2$ values of the various schemes of exchanges. The worst fits were clearly obtained when data were analyzed in schemes 1 and 4. The quality of the fit slightly but significantly improved in both schemes 5 and 6 (schemes 5b and 6b) when a small isolated compartment of $PCr_2$ was considered. The lowest min $\chi^2$ value was found in scheme 6b, indicating that three different CK fluxes (three ATP pools) and two PCr pools are most appropriate to describe our NMR data.

## Validation of the scheme of exchange involving three CK reactions

Until now, we considered the system as an exchange between different kinetic compartments. In the following, we propose a physical identification of the kinetic compartments (Table 4) and attempt to validate our schemes of exchange by comparing the fitted parameters with independent experimental determinations. The $ATP_2$ and $PCr_2$ pools were previously evidenced by an inversion transfer protocol with saturation of Pi resonance and identified as mitochondrial compartments by comparison with subcellular fractionation determination. Mitochondrial ATP amounted to $23 \pm 2\%$ of the total cellular content and PCr to $14 \pm 2\%$ at similar contractile performance. Due to both mitochondrial isolation procedure

and low cell contractility, the proportion of mitochondrial metabolites found in isolated cells or mitochondria (Asimakis and Sordahl, 1981; Geisbuhler et al., 1984) is lower than observed in a myocardium performing work as discussed previously (Joubert et al., 2001). ATP synthesis was 2.3 mmoles/l/s (as estimated from the measured oxygen consumption, $QO_2$). The comparison of experimental measurements (ATP synthesis and the size of mitochondrial pools) with the adjusted parameters (shown in Table 3) was used as an additional criterion of selection. Scheme 1 was rejected, because it did not consider ATP compartmentation. In scheme 2, 30% of the total ATP was completely isolated from the cellular energy exchanges: this is incompatible with the fact that 95% of cellular ATP is ultimately labeled by $^{18}$O through Pi (Zeleznikar et al., 1991). Scheme 3 was eliminated on the basis of a low mitochondrial ATP synthesis (Pi→$ATP_2$ = 0.1 mmoles/l/s), incompatible with the measured $QO_2$. Negligible or huge size of the mitochondrial ATP compartment allowed for rejection of schemes 4 and 5c, respectively. In all other schemes (5, 5b, 6, and 6b), the size of $ATP_2$ (ranging from 22 to 27% of the total ATP) was in agreement with the mitochondrial ATP compartment measured in a normoxic heart performing a medium work. On the basis of the conjunction of criteria, the lowest min $\chi^2$, and the adequacy of the fitted and measured parameters, scheme 6b appeared as the best minimal scheme describing energetic exchange in our conditions of contractility. Further, both the forward and reverse flux of mito-CK and MM-CK could be considered by imposing the ATP synthesis flux as an additional constraint. The mitochondrial forward flux (PCr→$ATP_2$) fell to zero (0.01 ± 0.29 mmole/l/s), which was not the case for the MM-CK reverse flux ($ATP_3$→PCr).

Until now, the equality of the intrinsic relaxation parameters in the subcellular compartments was imposed as a constraint. This constraint was released to evaluate its influence on the determination of the parameters and to estimate $T_1$ values in each compartment. In none of the schemes 2–5 the release of the constraint on $T_1$ equality significantly modified the parameters although their confidence interval markedly increased (not shown). In scheme 6b, because of the high number of variables, releasing $T_1$ equality could not be done without imposing a new constraint (for example the value of Pi→$ATP_2$ exchange). The following values of $T_1$ were obtained: $T_{1PCr1}$ = 5.5 ± 7.0 s; $T_{1PCr2}$ = 2.4 ± 4.1 s; $T_{1\gamma ATP1}$ = 0.8 ± 0.3 s; $T_{1\gamma ATP2}$ = 0.5 ± 0.4 s; $T_{1\gamma ATP3}$ = 0.2 ± 0.3 s (min $\chi^2$ was 153). Despite the high intervals of confidence, the $T_1$ of metabolites located in subcellular compartments had a tendency to be lower than in cytosol.

Thus, the best minimal model proposes three distinct kinetics of the CK reactions: 1) a cytosolic CK at equilibrium $PCr_1 \leftrightarrow ATP_1$, 2) a flux $PCr_1 \leftrightarrow ATP_3$, which might reflect MM-CK bound close to myofibrillar, sarcoplasmic reticulum, or sarcolemmal ATPases, and 3) a flux $ATP_2 \rightarrow PCr_1$, which might originate from mito-CK and translocase activities.

## DISCUSSION

The development of the new methodology presented here was motivated by two main questions. What is the origin of the discrepancy between the forward and reverse CK fluxes in the perfused heart, often observed in magnetization transfer experiments? Can $^{31}$P NMR spectroscopy give access to a specific information on the flux of the subcellular CK isoforms? We previously showed that neglecting in the analysis a mitochondrial metabolite compartment could explain the flux discrepancy in an inversion protocol under saturation of Pi (Joubert et al., 2000, 2001). However, this hypothesis was insufficient to fully account for all NMR data, particularly in the absence of Pi saturation. Using the simultaneous analysis of different protocols of magnetization transfer, we show here that it is necessary to use a kinetic scheme of analysis that takes into account the complex organization of the cell and the CK isoforms localization. The proximity of enzymes is known to influence their kinetics both in vitro (Arrio-Dupont et al., 1992) and in isolated mitochondria or skinned fibers of skeletal and cardiac muscles (Saks et al., 1985; Ventura-Clapier et al., 1987, 1994). Although the necessity of considering metabolic compartmentation in the NMR analysis has been previously questioned (McFarland et al., 1994), its importance was earlier proposed (Kupriyanov et al., 1984; Koretsky et al., 1985, 1986; Zahler et al., 1987; Zahler and Ingwall, 1992), but never directly demonstrated.

### Advantage of an integrated analysis approach

The interpretation of NMR magnetization transfer experiments, like that of any tracer experiment, is always dependent on the scheme of exchange used to analyze the data. In the case of the CK reactions, the hypothesis of cardiac cell homogeneity has been widely used in the NMR analysis. It implies a kinetic equivalence of the different CK and an unlimited diffusion of CK substrates. However, it is difficult, in a beating heart, to test the validity of these hypotheses using a single global magnetization transfer experiment. For instance, an ATP pool involved in mito-CK flux was early proposed (Zahler et al., 1987; Zahler and Ingwall, 1992), to account for the double exponential decrease of the PCr magnetization under saturation of γATP. However, the computation of mito-CK flux by the analysis of a unique saturation protocol, had to rely on several hypotheses (imposed values of ATPases flux, $T_{1PCr}$, and size of the ATP pool) and considered exclusively one scheme of exchange (two ATP pools exchanging with a PCr pool), neglecting the

compartment resulting from the vicinity of MM-CK with ATPases.

Our simultaneous analysis of several NMR experiments offers the opportunity to overcome these difficulties by increasing the amount of information. Indeed, whatever the magnetic perturbation is, each magnetic relaxation reflects the same kinetic properties. The adequate kinetic scheme describing the physiological exchange must thus account for the data of each magnetization transfer protocol. Using quantitative criteria, it becomes possible to test several models of exchange and to propose the most appropriate scheme accounting for NMR data of the four magnetization perturbations. The major advantage of this approach is that the analysis does not rely on a priori hypothesis on the size of subcellular compartments or restriction of metabolite diffusion. The consistency of the fitted values with those measured by other experimental approaches (fractionation, oxygen consumption) emphasizes the interest of the method.

## Origin of the CK flux discrepancy

The question of the CK flux discrepancy observed by magnetization transfer has often been addressed (Nunnally and Hollis, 1979; Meyer et al., 1982; Matthews et al., 1982; Bittl and Ingwall, 1985; Koretsky et al., 1985; Ugurbil et al., 1986; Spencer et al., 1988; Joubert et al., 2000, 2001). Several hypothesis were proposed but none could fully explain all the data. The influence of the ATP–Pi exchange on CK flux determination was proposed as a major experimental pitfall. The discrepancy between $F_f$ and $F_r$, previously observed by protocols of saturation, was abolished when the ATP–Pi exchange was masked by a continuous saturation of Pi (Ugurbil et al., 1986), although the importance of this exchange was questioned both experimentally (Koretsky et al. 1986; Joubert et al., 2000) and on theoretical ground (Brindle, 1988). Besides, saturation of Pi might not just eliminate the contribution of the ATP-Pi exchange, but might also affect other cellular reactions, as an exchange between PCr and mitochondrial ATP. Here we clearly confirmed that the exclusive hypothesis of an ATP-Pi exchange (three-site exchange proposed by Ugurbil et al., 1986) is insufficient to account for this apparent flux discrepancy. It means that, on kinetic grounds, a myocardial CK system cannot be considered as a "well mixed solution" as suggested in skeletal muscle (McFarland et al., 1994). The consideration of ATP and PCr intracellular pools ($ATP_2$ and $PCr_2$) improved the analysis (schemes 2–5c) although it was still insufficient to correctly describe the NMR data. Only schemes 6 and 6b, which consider the presence of three ATP pools and therefore the specific function of three CK (most likely mito-CK, cytosolic CK, and MM bound-CK), could account for the global expected CK flux equality. Scheme 6b, on the basis of its lowest min $\chi^2$, is further

discussed as the best predictive scheme of exchange for the myocardium at this level of activity.

This scheme is in agreement with the hypothesis of Korestky et al. (1985), suggesting that one (or several) small ATP pools exchanging with PCr could explain CK fluxes discrepancy. Indeed one of these pools ($ATP_3$) could fuel MM-CK in the vicinity of the myosin or of sarcolemmal or sarcoplamic reticulum ATPases. The size of the $ATP_2$ pool (22% of total) is compatible with the subcellular fractionation determination of mitochondrial ATP, which includes both the mitochondrial matrix and the inter-membrane space. A small part of $ATP_2$ in the inter-membrane space could indeed exchange with PCr through mito-CK, whereas another ATP fraction, the product of matricial ATP synthase ($Pi \rightarrow ATP_2$), would be transferred between the matrix and the inter-membrane space by the adenine nucleotide translocator. Thus, the exchange $ATP_2 \leftrightarrow PCr_1$ can be proposed to be a "black box" containing both the adenine nucleotide translocator and mito-CK fluxes.

On a theoretical ground, an exchange involving small metabolic pools was previously suggested to be undetectable by an inversion protocol (Koretsky et al., 1985). This was probably the case when a single protocol of inversion transfer was analyzed, but was not the case in our simultaneous analysis of four protocols that provided sufficient information to infer the presence of small compartments and their exchange fluxes. Indeed, even if the small pools were not directly observable, the influence of their exchange on the other compartments could be detected.

## Bioenergetic considerations

Our work was concerned by the development of an experimental methodology to obtain specific information on subcellular energetic exchanges. This problem is crucial inasmuch as the different CK isoforms, due to their vicinity with other enzymes, may be regulated in different ways and play distinct roles (Saks et al., 1996). Indeed, several mathematical models have been proposed to evaluate the subcellular CK fluxes and their role in the whole organ (Aliev and Saks, 1997; Kemp et al., 1998; Vendelin et al., 2000; Jeneson et al., 2000). Such theoretical approaches always relied on several assumptions (for example, the structure of the scheme, the metabolite concentration in subcellular compartments, a restriction of metabolite diffusion, the kinetic behavior of CK isoforms in situ, etc.). We believe that our approach is able to bring experimental validation of this theoretical analysis of subcellular energy exchanges. Indeed the power of this strategy is that the analysis of NMR data does not require any of these assumptions.

The comparative analysis of min $\chi^2$ presented in Fig. 3 clearly rejects two exchange schemes and supports the following conclusions. The myocardial cell cannot be described as a homogenous distribution of metabolites and

enzymes (Scheme 1). The consideration of three different CK functioning appears to best fit the whole experimental data at this level of cardiac work. The best exchange scheme describing our control hearts is compatible with the hypothesis of a strict PCr-Cr-CK shuttle, as initially proposed by Bessman and Geiger (1981). The transport of energy from sites of energy production (mitochondria) to sites of ATP utilization occurs via PCr diffusion and conversion through the different CK isozymes. Clearly an exclusive diffusion flux of ATP between mitochondria and cytosol (scheme 4) was inadequate. However, due to the high number of unknown parameters, it was impossible to simultaneously obtain information on both the direct transport of ATP from mitochondria to cytosol and its transfer through mito-CK flux, and we cannot exclude the existence of a small direct ATP transport. The progression toward such precise information will come from other sources of data.

In conclusion, this is the first study showing that NMR magnetization transfer protocols are able to bring direct information on the kinetics of the subcellular CK isoforms in a whole organ without requiring an information on the substrates concentrations in the vicinity of these isoenzymes. In the adult heart function, a minimal scheme fully accounting for NMR data implies the consideration of three different CK kinetics and confirms the importance of subcellular compartmentation. This new experimental approach opens the possibility of a quantification of metabolites in specific subcellular sites of interest. Furthermore, it looks very promising to study the modifications of the subcellular energy circuit in relation to myocardial contractility in patho-physiological situations. The pathways describing subcellular fluxes of energy exchange might indeed vary according to patho-physiological conditions (i.e., the level of work, the myocardial substrate, the expression of the various isoenzymes, etc.). It is therefore expected that changing the ATP demand or synthesis will affect the distribution of the pathways of energy transfer. In other words, the control strength of the mito-CK pathway is expected to vary with the activity of the system. Besides, this strategy is not limited to its NMR present application: additional pathways can be investigated using other tracers ($^{18}$O, $^{13}$C, or $^{1}$H). Furthermore, it can be generalized to any kind of kinetic data allowing evaluation of the function of cell compartmentation.

## REFERENCES

Aliev, M. K., and V. A. Saks. 1997. Compartmentalized energy transfer in cardiomyocytes: use of mathematical modeling for the analysis of in vivo regulation of respiration. *Biophys. J.* 73:428–445.

Arrio-Dupont, M., J.-J. Bechet, and A. D'Albis. 1992. A model system of coupled activity of co-immobilized creatine kinase and myosin. *Eur. J. Biochem.* 207:951–955.

Asimakis, G. K., and L. A. Sordahl. 1981. Intramitochondrial adenine nucleotides and energy linked functions in heart mitochondria. *Am. J. Physiol. Heart Circ. Physiol.* 241:H672–H678.

Bessman, S. P., and P. J. Geiger. 1981. Transport of energy in muscle: the phosphorylcreatine shuttle. *Science.* 211:448–452.

Bittl, J. A., and J. S. Ingwall. 1985. Reaction rates of creatine kinase and ATP synthesis in the isolated rat heart. A $^{31}$P NMR magnetization transfer study. *J. Biol. Chem.* 260:3512–3517.

Brindle, K. M. 1988. NMR methods for measuring enzyme kinetics in vivo. *Prog. NMR Spectrosc.* 20:257–293.

Geisbuhler, T., R. A. Altschuld, R. W. Trewyn, A. Z. Ansel, K. Lamka, and G. P. Brierley. 1984. Adenine nucleotide metabolism and compartmentalization in isolated adult rat heart cells. *Circ. Res.* 54:536–546.

Hoerter, J. A., C. Lauer, G. Vassort, and M. Guéron. 1988. Sustained function of normoxic hearts depleted in ATP and phosphocreatine: a $^{31}$P NMR study. *Am. J. Physiol. Cell Physiol.* 255:C192–C201.

Jeneson, J. A., H. V. Westerhoff, and M. J. Kushmerick. 2000. A metabolic control analysis of kinetic controls in ATP free energy metabolism in contracting skeletal muscle. *Am. J. Physiol. Cell Physiol.* 279: C813–C832.

Joubert, F., B. Gillet, J.-L. Mazet, P. Mateo, J.-C. Beloeil, and J. A. Hoerter. 2000. Evidence for myocardial ATP compartmentation from NMR inversion transfer analysis of creatine kinase fluxes. *Biophys. J.* 79:1–13.

Joubert, F., I. Vrezas, P. Mateo, B. Gillet, J.-C. Beloeil, S. Soboll, and J. A. Hoerter. 2001. Cardiac creatine kinase compartments revealed by NMR magnetization transfer spectroscopy and subcellular fractionation. *Biochemistry.* 40:2129–2137.

Kemp, G. J., D. N. Manners, J. F. Clark, M. E. Bastin, and G. K. Radda. 1998. Theoretical modelling of some spatial and temporal aspects of the mitochondrion/creatine kinase/myofibril system in muscle. *Mol. Cell. Biochem.* 184:249–289.

Koretsky, A. P., V. J. Basus, T. L. James, M. P. Klein, and M. W. Weiner. 1985. Detection of exchange reactions involving small metabolite pools using NMR magnetization transfer techniques: relevance to subcellular compartmentation of creatine kinase. *Mag. Res. Med.* 2:586–594.

Koretsky, A. P., S. Wang, M. P. Klein, T. L. James, and M. W. Weiner. 1986. $^{31}$P NMR saturation measurements of phosphorus exchange reactions in rat heart and kidney in situ. *Biochemistry.* 25:77–84.

Kupriyanov, V. V., A. Y. Steinschneider, E. K. Ruuge, V. I. Kapel'ko, M. Y. Zueva, V. L. Lakomkin, V. N. Smirnov, and V. A. Saks. 1984. Regulation of energy flux through the creatine kinase reaction in vitro and in perfused rat heart. *Biochem. Biophys. Acta.* 805:319–331.

Matthews, P. M., J. L. Bland, D. G. Gadian, and G. K. Radda. 1982. A $^{31}$P NMR saturation transfer study of the regulation of creatine kinase in the rat heart. *Biochem. Biophys. Acta.* 721:312–320.

McConnell, H. M. 1958. Reaction rates by nuclear magnetization resonance. *J. Chem. Phys.* 28:430–431.

McFarland, E. W., M. J. Kushmerick, and T. S. Moerland. 1994. Activity of creatine kinase in a contracting mammalian muscle of uniform fiber type. *Biophys. J.* 67:1912–1924.

Meyer, R. A., M. J. Kushmerick, and T. R. Brown. 1982. Application of $^{31}$P-NMR spectroscopy to the study of striated muscle metabolism. *Am. J. Physiol. Cell Physiol.* 242:C1–C11.

Nunnally, R. L., and D. P. Hollis. 1979. Adenosine triphosphate compartmentation in living hearts: a phosphorus magnetic resonance saturation transfer study. *Biochemistry.* 18:3642–3646.

Press, W. H., S. A. Teukolsky, W. T. Vettterling, and B. P. Flannery. 1994. Numerical recipes in Fortran. The art of scientific computing. Cambridge Univ. Press, Cambridge, U.K. 678–682.

Saks, V. A., A. V. Kuznetsov, V. V. Kupriyanov, M. V. Micelli, and W. E. Jacobus. 1985. Creatine kinase of rat heart mitochondria. The demonstration of functional to oxidative phosphorylation in an inner membrane-matrix preparation. *J. Biol. Chem.* 260:7757–7764.

Saks, V. A., R. Ventura-Clapier, and M. K. Aliev. 1996. Metabolic control and metabolic capacity: two aspects of creatine kinase functioning in the cells. *Biophys. Biochim. Acta.* 1274:81–88.

Spencer, R. G., J. A. Balschi, J. S. Leigh, and J. S. Ingwall. 1988. ATP synthesis and degradation rates in the perfused rat heart. [31]P nuclear magnetization resonance double saturation transfer measurements. *Biophys. J.* 54:921–929.

Stepanov, V. P., P. Mateo, B. Gillet, J.-C. Beloeil, and J. A. Hoerter. 1997. Kinetics of creatine kinase in an experimental model of low phosphocreatine and ATP in the normoxic heart. *Am. J. Physiol. Cell Physiol.* 273:C1397–C1408.

Ugurbil, K., M. A. Petein, R. Maiden, S. P. Michurski, and A. H. L. From. 1986. Measurement of an individual rate constant in the presence of multiple exchanges: Application to creatine kinase rates. *Biochemistry.* 25:100–108.

Vendelin, M., O. Kongas, and V. A. Saks. 2000. Regulation of mitochondrial respiration in heart cells analyzed by reaction–diffusion model of energy transfer. *Am. J. Physiol. Cell Physiol.* 278:C747–C764.

Ventura-Clapier, R., V. A. Saks, G. Vassort, C. Lauer, and G. V. Elizarova. 1987. Reversible MM-creatine kinase binding to cardiac myofibrils. *Am. J. Physiol. Cell Physiol.* 253:C444–C455.

Ventura-Clapier, R., V. Veksler, and J. A. Hoerter. 1994. Myofibrillar creatine kinase and cardiac contraction. *Mol. Cell. Biochem.* 133: 125–144.

Wallimann, T., M. Wyss, D. Brdiczka, K. Nicolay, and H. M. Eppenberger. 1992. Intracellular compartmentation, structure and function of creatine kinase isoenzymes in tissues with high and fluctuating energy demands —the phosphocreatine circuit for cellular energy homeostasis. *Biochem. J.* 281:21–40.

Wallimann, T. 1996. ^{31}P-NMR-measured creatine kinase reaction flux in muscle: a caveat! *J. Muscle Res. Cell. Motil.* 17:177–181.

Zahler, R., J. A. Bittl, and J. S. Ingwall. 1987. Analysis of compartment of ATP in skeletal and cardiac muscle using ^{31}P nuclear magnetic resonance saturation transfer. *Biophys. J.* 51:883–893.

Zahler, R., and J. S. Ingwall. 1992. Estimation of heart mitochondrial creatine kinase flux using magnetization transfer NMR spectroscopy. *Am. J. Physiol. Heart Circ. Physiol.* 262:H1022–H1028.

Zeleznikar, R. J., and N. D. Goldberg. 1991. Kinetics and compartmentation of energy metabolism in intact skeletal muscle determined from [18]O labeling of metabolite phosphoryls. *J. Biol. Chem.* 266: 15110–15119.